RSC Advances

PAPER

View Article Online
View Journal | View Issue

Cite this: *RSC Adv.*, 2017, **7**, 30128

Regio- and stereoselective synthesis of novel isoxazolidine heterocycles by 1,3-dipolar cycloaddition between *C*-phenyl-*N*-methylnitrone and substituted alkenes. Experimental and DFT investigation of selectivity and mechanism†

Djamila Hellel,[a] Fouad Chafaa,[a] Abdelmalek Khorief Nacereddine,[ab]* Abdelhafid Djerourou[a] and Emmanuel Vrancken[c]

A series of isoxazolidine heterocycles was synthesized through the 1,3-dipolar cycloaddition (13DC) reaction of *C*-phenyl-*N*-methylnitrone with different substituted alkenes. The structures and stereochemistry of the cycloadducts were determined by spectroscopic methods. These 13DC reactions are characterized by complete regioselectivity and high stereoselectivity. The molecular mechanism, reactivity and selectivity of these 13DC reactions have been investigated by means of transition state theory and reactivity indices derived from conceptual DFT using DFT methods at the B3LYP/6-31G(d,p) level of theory. The obtained results indicate that these cycloaddition reactions take place through a one-step synchronous mechanism with a non-polar mechanism and high activation energies. The theoretical results are in agreement with the experimental findings.

Received 7th January 2017
Accepted 15th May 2017

DOI: 10.1039/c7ra00258k

rsc.li/rsc-advances

1. Introduction

The 1,3-dipolar cycloaddition (13DC) reaction is one of the most useful reactions in organic synthesis.[1] Many dipoles and dipolarophiles have been employed to obtain either carbocyclic or heterocycles compounds with both oxygen and nitrogen atoms.[2] Nitrones are a class of powerful reagents, which readily undergo 13DC with various dipolarophiles, in particular with alkenes to afford in high yields important isoxazolidines (Scheme 1).[3] These cycloadducts have attracted considerable attention due to their potential biological activities, have been used as precursors for β-amino alcohols through reductive cleavage of the N–O bond, and have been considered as potential precursors for the synthesis of many natural products such as β-lactam antibiotics, alkaloids,[4] and especially sugar and nucleoside analogues.[5] Isoxazolidines possess medicinal activities such as antibacterial, anticonvulsant, antibiotic, antitubercular and antifungal activities[5]

A tremendous number of experimental and theoretical works can be found in the literature devoted to the study of the 13DC reaction of nitrones with alkenes for the synthesis of isoxazolidines.[6] Tran *et al.*[7] experimentally studied the 13DC reaction between *C*-phenyl-*N*-methylnitrone and dimethyl 2-benzylidenecyclopropane-1,1-dicarboxylate finding that this reaction is regio- and stereoselective yielding the corresponding *ortho*/*endo* cycloadduct as a single regio- and stereocycloadduct (Scheme 2). In order to explain the observed regio- and stereoselectivities, we have studied recently this 13DC reaction finding the formation of a non-classical hydrogen bond (HB) between the carbonyl oxygen atom of one of the two carboxylate groups of alkene and the nitrone C3–**H** hydrogen atom (Fig. 1). Formation of this non-classical HB, provokes a stabilization by 7 kcal mol^{-1} and can overcome the low *meta* regioselectivity.[8]

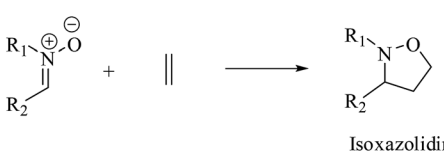

Scheme 1 Synthesis of isoxazolidines by 13DC reaction of nitrones with simplest ethylene.

[a]*Laboratoire de Synthèse et Biocatalyse Organique, Département de Chimie, Faculté des Sciences, Université Badji Mokhtar Annaba, BP 12, 23000 Annaba, Algeria. E-mail: khorief.abdelmalek@univ-annaba.org*

[b]*Département de Physique et Chimie, Ecole Normale Supérieure d'Enseignement Technologique de Skikda, Cité des frères Boucetta, Azzaba, Skikda, Algeria*

[c]*Institut Charles Gerhardt, UMR 5253 CNRS-UM2-UM1 ENSCM, Laboratoire Architectures Moléculaires et Matériaux Nanostructurés (AM2N), Ecole Nationale Supérieure de Chimie de Montpellier, 8 Rue de l'Ecole Normale, 34296 Montpellier, France*

† Electronic supplementary information (ESI) available. See DOI: 10.1039/c7ra00258k

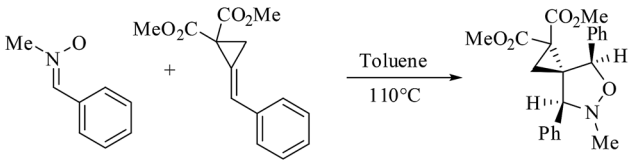

Scheme 2 13DC reaction between *C*-phenyl-*N*-methylnitrone and dimethyl 2-benzylidenecyclopropane-1,1-dicarboxylate.

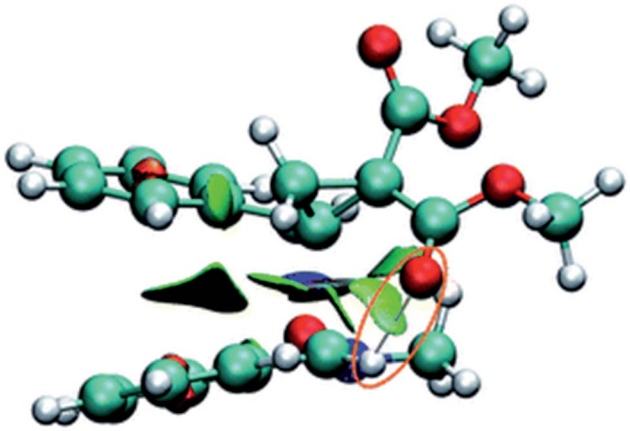

Fig. 1 Non-classical HB at the *meta–endo* approach.

Recently, Falkowska and co-workers[9] reported the synthesis of SF_5-substituted isoxazolidines which prepared in moderate yields by 13DC reactions between pentafluorosulfanyl-substituted acrylic ester or amides with nitrones as dipoles (Scheme 3). The authors have founds from his theoretical study that the selectivity of this 13DC reaction is a result of the balance between two sterical interactions, in which the sterical bulkiness of substituent *Z* is predominant, SF_5-*endo*-approaches will be favored conducting to a mixture of diastereoisomers. On the contrary, minimizing the steric effect with SF_5 will conduct to 3,4-*trans* diastereoisomer.

From the literature, we can note that the regio- and stereoselectives of cycloaddition reaction and namely 13DC are mainly controlled by the electronic and steric factors of the substituent at the dipole or at the dipolarophile. Despite that there are many theoretical approaches that can predict the regioselectivity; such as the Houk's rule based on FMO analysis[10] and the DFT-based reactivity indices,[11] the stereoselectivity is often generally reliant to the steric effects of the

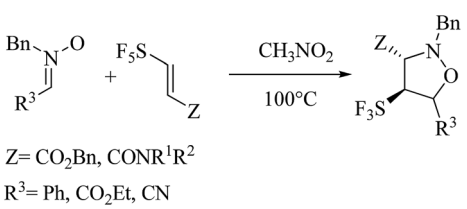

Scheme 3 13DC reaction between pentafluorosulfanyl-substituted acrylic ester and amides with nitrones reported by Falkowska.[9]

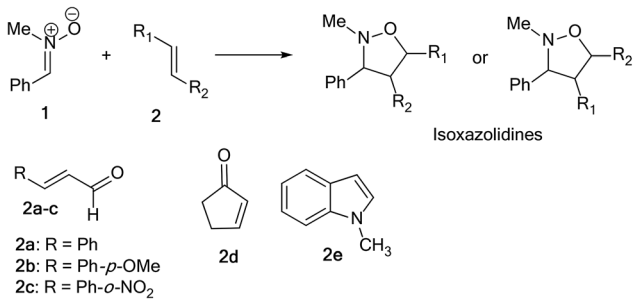

Scheme 4 13DC reaction between nitrone **1** and dipolarophiles **2a–e**.

substituent, alike, in many cases, when the reactants possess a voluminous substituent's, the regioselectivity cannot be predicted using these theoretical models. Thereby, it is necessary to study each reaction as a separate system.

Herein, we focused to perform an experimental as well as theoretical studies of the 13DC reactions between nitrone **1** prepared previously as dipole with various substituted alkenes **2a–e** as a dipolarophiles leading to the formation of the corresponding isoxazolidines (Scheme 4) in order to shed light on the factors that controlled the regio- and stereoselectivities, as well as the molecular mechanism of these 13DC reactions.

2. Results and discussion

The present study has been divided into two dependent parts; in the first part, the synthesis of isoxazolidines heterocycles using 13DC reactions between nitrone **1** and a series of alkenes **2a–e** were performed and the structure of cycloadducts was characterized using spectroscopic usual methods (IR, NMR and MS). In the second part, we have performed a theoretical analysis using DFT methods of the regio- and stereoselectivities observed in the Experimental part as well as the molecular mechanism using theoretical approaches such as transition state theorem[12] and reactivity indices defined within the context of the conceptual DFT.[13]

2.1. Experimental part

In order to synthesize the isoxazolidines heterocycles, we envisaged to prepare in first place the nitrone **1** which is easily accessible from the condensation reaction between benzaldehyde and the *N*-methyl-hydroxylamine-hydrochloride (Scheme 5). This nitrone has been obtained according to the procedure reported in literature,[14] in which its structure was determined by spectroscopic methods (IR, NMR and mass). The

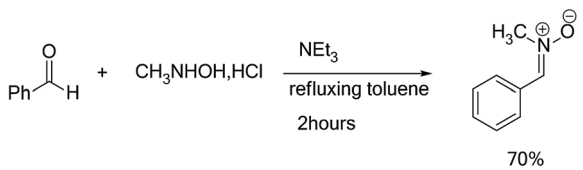

Scheme 5 Synthesis of nitrone **1**.

Table 1 Experimental results of 13DC reactions between nitrone **1** and alkenes **2a–e**

Alkene	Time (h)	Yield (%)	Cycloadduct
2a	24	10	**CA-a-mn** (100%)
2b	24	12	**CA-b-mn** (100%)
2c	24	49	**CA-c-mn** (80%)
			CA-c-mx (20%)
2d	08	90	**CA-d-mx** (100%)
2e	12	23	**CA-e-ox** (100%)

13DC reaction of nitrone **1** with the set of alkenes **2a–e** were performed under refluxing polar solvent (toluene) at 110 °C in order to enhance the reactivity of both nitrone and alkenes. In the case of alkenes **2a**, **2b** and **2e**, the corresponding isoxazolidines were obtained in a low yields 10, 12 and 23%, respectively (Table 1: entries 1, 2 and 5). Increasing the time of reaction or heating at 130 °C for 20 hours did not improve the yield. On the other hand, the 13DC reaction of nitrone **1** with both alkenes **2c** and **2d** leading to the formation of the corresponding isoxazolidines cycloadducts in a moderate (49%) and good yields (90%), respectively (see Table 1: entries 3 and 4). The slight increase in the yield can be explained by the presence of an electron-withdrawing group (NO_2) at the alkene **2c** which enhance the reactivity of the alkene to become a good electrophile.

The structural determination of isoxazolidines **3a–e** has been performed spectroscopically using usual methods such as IR, NMR and MS spectrums. In the case of isoxazolidines **3a** and **3b**, only one regioisomer (*meta*) and one diastereoisomer (*trans*) is observed. The assigned structures are again based on rigorous spectroscopic analysis for NMR data. The structure of different stereoisomers has been determined from coupling constant of selected hydrogens at the ^{1}H NMR spectrum according to the data reported in the literature.[15] Thus, the value of coupling constant of the hydrogens in position *cis* (J > 6 Hz) is always higher than that of hydrogens *trans* (J < 6 Hz).

The 13DC reaction between nitrone **1** and alkene **2c** processed with completely *meta* regioselectivity and leads to the formation of a mixture of two diastereoisomers (*trans*/*cis*) in a ratio of 80 : 20 (see Table 1, entry 3). Note that the diastereoisomeric ratio was determined by integration of the corresponding ^{1}H NMR signals of the crude mixture spectrum.

The two-dimensional NMR (^{1}H–^{1}H and ^{1}H–^{13}C) and HRMS analysis has been also used to confirm the structures of the obtained compounds.

Using the same reaction conditions (Scheme 6), the alkene **2d** reacts with the nitrone **1** during 8 hours to give a single regio- and diastereoisomer cycloadduct in a good yield (90%). However, in the case of the alkene **2e** (Scheme 6), this 13DC reaction leads to the formation of a single regio- and stereoisomer in a poor yield (23%), for 12 hours of time (see Table 1, entry 5). This fact may be explained by the effects electronic donating of the conjugate nitrogen atom witch make the alkene **2e** electron-rich ethylene, and thereby, it reacts as a nucleophile with nitrone **1** that it is naturally classified as a nucleophile species. Therefore, this 13DC become requiring strong experimental reaction conditions such as hard heating or high pressure, which explain the obtained low yield.

The obtained regioisomers (*ortho*/*meta*) were determined from cosy ^{1}H/^{1}H spectrum. On the other hand, the stereoisomers (*trans*/*cis*) determination has been performed using hydrogen coupling constants (J), which were extracted from the ^{1}H NMR spectrum. The assigned regiochemistry of isoxazolidines **2a**, **2b**

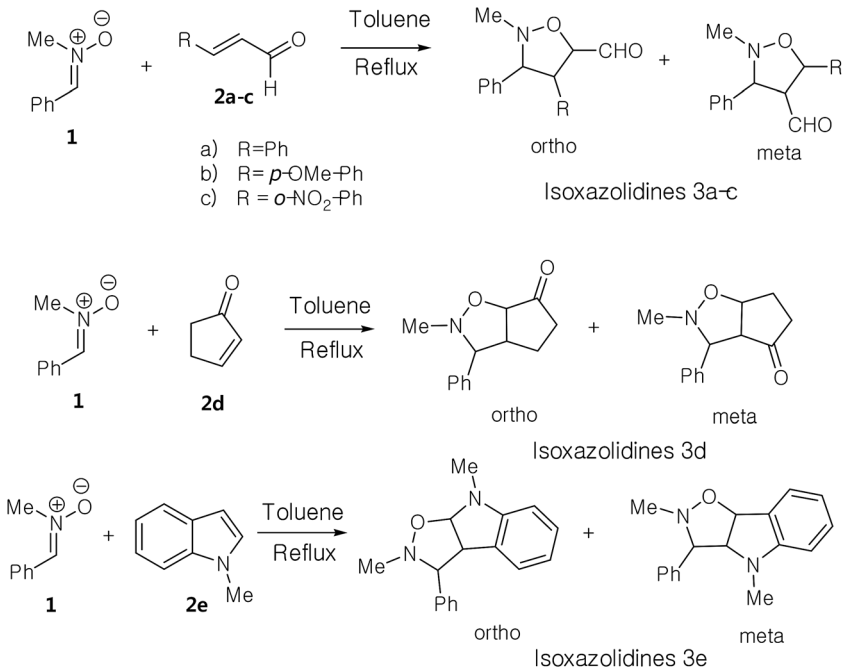

Scheme 6 Synthesis of isoxazolidines *via* 13DC reaction of nitrone **1** with alkenes **2a–e**.

and **2c** is based on the chemical shift value and multiplicity of C4–**H**. The *trans*/*cis* or *endo*/*exo* determination between C3–**H** and C4–**H** and between C4–**H** and C5–**H** are based on the value of coupling constant ^{1}H NMR, using the rule that *cis* vicinal ^{1}H coupling constant are always higher (5–9 Hz) than that of *trans* (0–5 Hz) in case of isoxazolidines and related heterocycles.[15]

The analysis of NMR cosy spectra of isoxazolidines **3a**, **3b** and **3c** shows that the signal of the proton C4–**H** at δ 3.38 ppm appear as multiplet which is coupled with the protons C3–**H** and C5–**H** and is also coupled with the proton of the aldehyde function (C**H**O) which is appear in the range from δ 8–10 ppm (Scheme 7). Therefore, the isoxazolidines cycloadducts **3a**, **3b** and **3c**, are a regioisomers *meta*. For the isoxazolidines **3d**, the signal of C4–**H** appear as a multiplet at δ 2.90 ppm is also coupled with the C3–**H** that is appear as a doublet at δ 3.42 ppm and with C5–**H** that is appear as multiplet at δ 4.86 ppm. Thereby, the obtained isoxazolidines is the *meta* regioisomer.

For the isoxazolidine **3e**, the obtained cycloadduct is an *ortho* regioisomer, because the proton C5–**H** appears in a low intensity, this fact is due to the electron withdrawing effects of two electro-attractor atoms; oxygen and nitrogen. Thereby, the signal of C5 and C5–**H** atoms appear in low values of chemical shifts. Furthermore, this hydrogen appears as a doublet because it coupled only with the C4–**H**. The assigned ^{13}C chemical shift values are in consonance with the assigned structures of isoxazolidines **3a–e**.

For the isoxazolidines **3e**, the low coupling constant of the C3–**H** with C4–**H** ($J \approx 0$ Hz), being indicative that the C3–**H** and the C4–**H** are in *trans* relationship, based on the value obtained in the isoxazolidines heterocycles.[15] Consequently, the stereochemistry of isoxazolidines **3e** is *ortho–trans* or *ortho–exo* (see Scheme 7).

For, isoxazolidine **3a**, the coupling constant $J_{3,4} = 3.68$ Hz account for a *trans* relationship between C3–**H** and C4–**H**. In addition the coupling constant $J_{5,4} = 5.8$ Hz indicated that the C4–**H** and C5–**H** are in *trans* position (see Scheme 7). The same reasoning in the case of isoxazolidine **3b**, in which the low values of coupling constants $J_{3,4} = 3.68$ Hz and $J_{5,4} = 5.8$ Hz indicative for the *trans* relationship between them and leading to predict the structure shown in Scheme 7.

For the isoxazolidine **3c**, the apparition of two signals adjacent with different integrations in the ^{1}H NMR spectrum of the crude product for the C5–**H** indicative for the formation of a mixture of two diastereoisomers, in which one appears at δ 5.90 as doublet ($J = 12$ Hz) and the second also as a doublet at δ 5.95 ($J = 4$ Hz). From the value of coupling constants, these values indicative for a *cis*-diastereoisomer for signal at 5.90 ppm and a *trans*-diastereoisomer for a signal at δ 5.95 ppm. The proportion calculation shown that the *trans*-diastereoisomer formed in a major amount (80%), whereas, the *cis*-diastereoisomer is the minor (20%).

From these results, we can note that the presence of a electron withdrawing group at the alkene favour the formation of a *meta* regioisomers, however, the electron-donating group favor the *ortho* regioisomers. The *exo* stereoselectivity observed in these 13DC reactions may be attributed to steric factors.

2.2. Computational part

In this part, we have planned to study theoretically the effects of electronic and steric factors on the determination of the regio- and stereoselectivities as well as the nature of molecular mechanism. Therefore, we have chosen the alkenes **2a**, **2d** and **2e**, which the first has a planner structure and the others having an electron withdrawing and donating group, respectively.

2.2.1. Study of the 13DC reaction between nitrone 1 and alkene 2a. The 13DC reaction between nitrone **1** and alkene **2a** (Scheme 8) can proceeds *via* two regioisomeric channels (*ortho* and *meta*) and two stereoisomeric approaches (*endo* and *exo*). Consequently, four cycloadducts and the corresponding four transition states have been located and characterized. Scheme 9 show the possible regio- and stereoselective pathways together with the values of the relative energies of the transition states

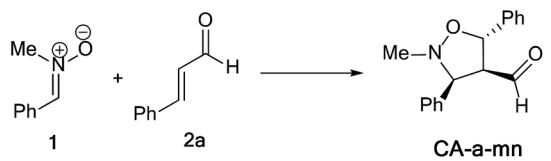

Scheme 8 13DC reaction between nitrones **1** and alkene **2a**.

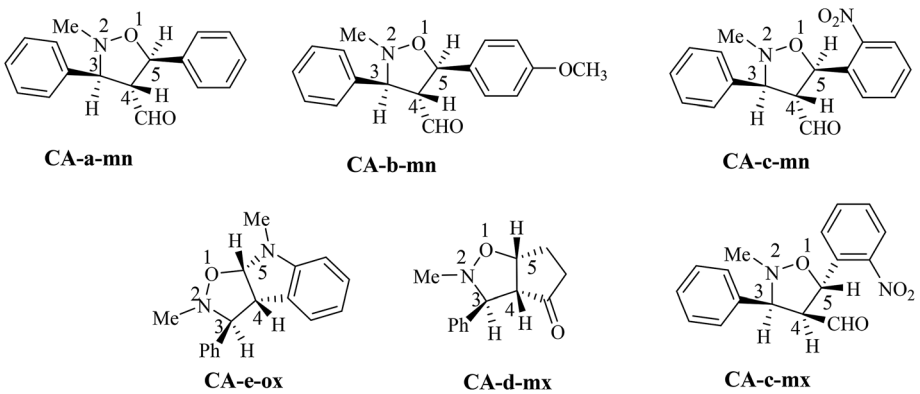

Scheme 7 Stereochemistry of the obtained cycloadducts of the 13DC reaction of nitrone **1** with alkenes **2a–e**.

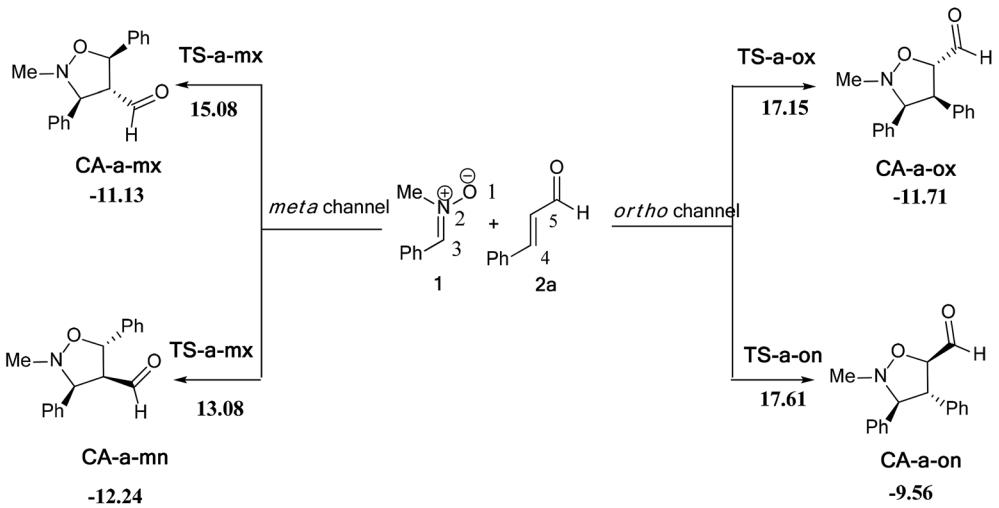

Scheme 9 The possible regio- and stereoisomeric pathways for the 13DC reaction of nitrone **1** with alkene **2a**.

(TSs) and cycloadducts, while relative energy profiles for the four possible pathways are given in Fig. 2. Total and relative energies of all stationary points involved in this 13DC reaction, in gas phase are gathered in Table S1 in ESI.†

The activation energies associated with this 13DC reaction are 13.08 (**TS-a-mn**), 15.08 (**TS-a-mx**), 17.61 (**TS-a-on**) and 17.15 kcal mol^{-1} (**TS-a-ox**). These values indicates that **TS-a-mn** is more favored by 2.00 kcal mol^{-1} than the second favored approach (**TS-a-mx**) and by 4.06 kcal mol^{-1} than the more favoured *ortho* approach (**TS-a-ox**), account for the complete *meta* regioselectivity and *endo* stereoselectivity. Moreover, the former cycloadducts are slightly stables between −9.56 and −12.24 kcal mol^{-1}, which account for the reversibility of this 13DC reaction, where, the **CA-a-mn** is the more stable one (ΔE = −12.24 kcal mol^{-1}). Therefore, the 13DC reaction between nitrone **1** and alkene **2a** favors kinetically and thermodynamically the formation of a single stereoisomer (**CA-a-mn**) generated from *meta–exo* approach, in great agreement with our experimental observation.

Values of relative enthalpies, entropies, and Gibbs free energies of the TSs and CAs involved in the 13DC reaction of nitrone **1** with alkene **2a** are displayed in Table 2, while total ones are collected in Table S2 in ESI.†

Inclusion of thermal corrections to the electronic energies increases the relative enthalpies of the TSs and CAs in the borderline of 2 kcal mol^{-1} (see Table 2), which remaining **TS-a-mn** (ΔH = 15.08 kcal mol^{-1}) the more favoured approach and the corresponding cycloadduct **CA-a-mn** (ΔH = −7.40 kcal mol^{-1}) the more stable one. Addition of the entropic contribution to the enthalpy increases dramatically the activation Gibbs free energy to 33.06, 34.89, 37.45 and 37.35 kcal mol^{-1} for **TS-a-mn**, **TS-a-mx**, **TS-a-on** and **TS-a-ox**, respectively, but does not changes the regio- and stereoselectivities. This fact is a consequence of the of the unfavorable activation entropy associated with these bimolecular processes. In addition, the process becomes slightly endothermic, account for the reversibility of this 13DC reaction, which explains the experimental low yield. The reversibility of this 13DC reaction indicates that it is also under thermodynamic control, in which

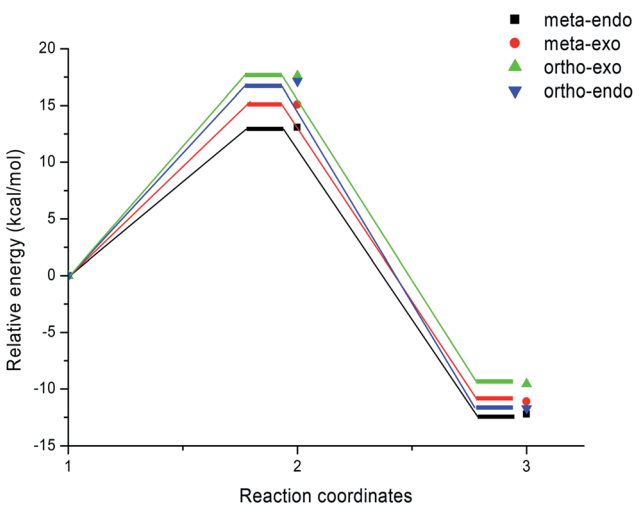

Fig. 2 Energy profiles for the competitive reactive pathways associated with the 13DC reaction between nitrone **1** and alkene **2a**.

Table 2 B3LYP/6-31G(d) relative enthalpies (ΔH, in kcal mol^{-1}), entropies (ΔS, in cal mol^{-1} K^{-1}) and Gibbs free energies (ΔG, in kcal mol^{-1}), for the TSs and CAs involved in the 13DC between nitrone **1** and alkene **2a**

	ΔH	ΔS	ΔG
TS-a-mn	15.08	−46.921	33.06
TS-a-mx	17.17	−46.257	34.89
TS-a-on	19.21	−47.614	37.45
TS-a-ox	19.18	−47.426	37.35
CA-a-mn	−7.40	−46.816	10.53
CA-a-mx	−6.27	−46.538	11.56
CA-a-on	−4.61	−48.899	14.13
CA-a-ox	−6.69	−46.947	11.30

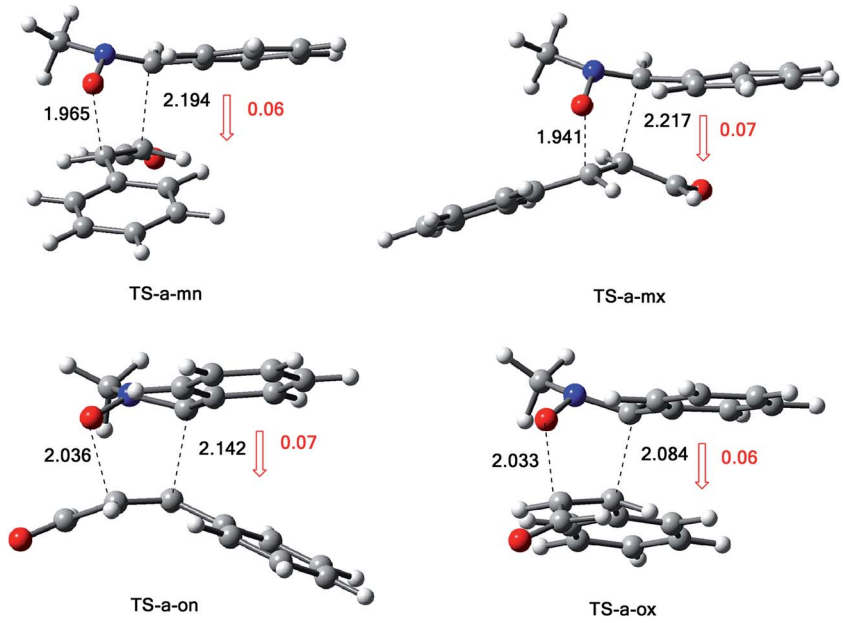

Fig. 3 Structure of TSs involved in the 13DC reaction between nitrone **1** and alkene **2a**.

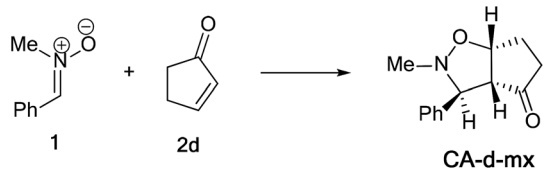

Scheme 10 13DC reaction between nitrone **1** and alkene **2d**.

CA-a-mn is favoured both kinetically and thermodynamically (more stable one).

The structures of the TSs involved in the 13DC reaction between nitrone **1** and alkene **2a** are given in Fig. 3. For the *meta* regioisomeric pathways, the lengths of the newly formed bonds O–C and C–C are 1.965 and 2.194 Å at **TS-d-mn**, 1.941 and 2.217 Å at **TS-d-mx**. For the *ortho* pathways, the lengths of the O–C and C–C new forming bonds are 2.036 and 2.142 Å at **TS-d-on** and 2.033 and 2.084 Å at **TS-d-ox**. These values indicate that at the *ortho* pathways the formation of O–C and C–C were performed synchronously. However, for the *meta* pathways, the formation of O–C and C–C were performed asynchronously; where, the new O–C σ bond is more advanced than the C–C one.

The polarity of this 13DC reaction has been analyzed by computing the global electron density transfer (GEDT) at the TSs. Along a polar reaction there is an electron-density transfer from the nucleophile partner toward the electrophile partner. This transfer can be analyzed through the GEDT value, in which, the high value of the GEDT at the TSs indicate for the high polar character of the reaction.

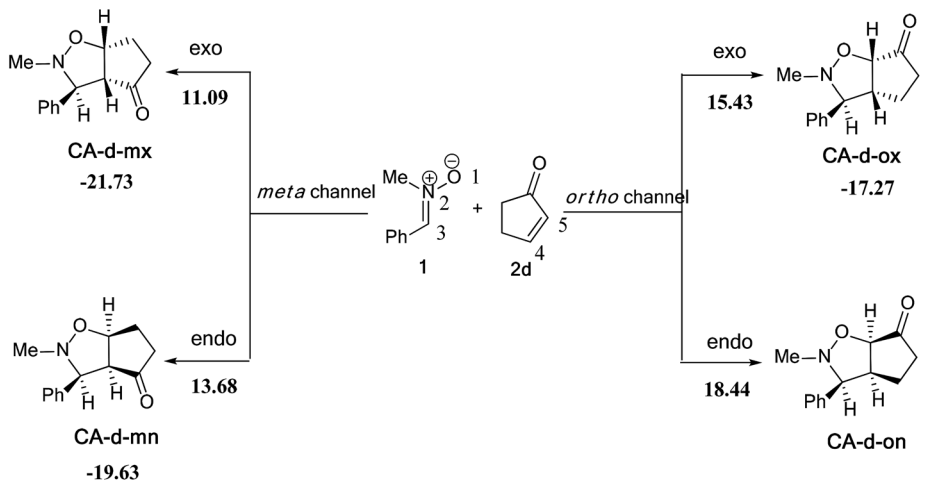

Scheme 11 The possible regio- and stereoisomeric pathways for the 13DC reaction of nitrone **1** with alkene **2d**.

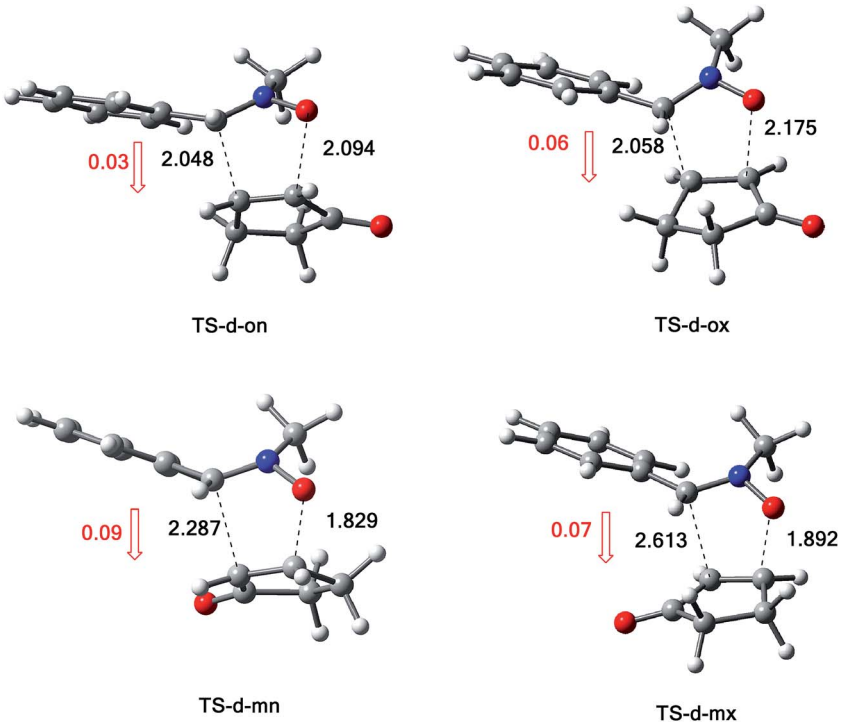

Fig. 4 Structure of TSs involved in the 13DC reaction between nitrone **1** and alkene **2d**.

The GEDT along these possible pathways using Natural Population Analysis (NPA).[16] The natural atomic charges at the TSs were calculated from the residual charge at the alkene **2a**. The negative sign of the GEDT account that the flux of GEDT takes place from nitrone **1** toward alkene **2a**. Therefore, nitrone **1** is considered as a nucleophile, whereas, alkene **2a** as an electrophile. The values of GEDT are 0.06*e* at **TS-a-ox**, 0.07*e* at **TS-a-on**, 0.07*e* at **TS-a-mx** and 0.06*e* at **TS-a-mn**. These low values accounts for a non-polar character for this 13DC reaction, justifying the obtained high activation energies and the experimental low yield.

2.2.2. Study of the 13DC reaction between nitrone 1 and alkene 2d. The 13DC reaction between nitrone **1** and alkene **2d**. was studied in this part (Scheme 10). This 13DC can proceeds *via* two regioisomeric channels (*ortho* and *meta*) and two stereoisomeric approaches (*endo* and *exo*). Consequently, four cycloadducts and the corresponding four transition states were been located and characterized (Scheme 11). Values of the total and relative energies of the stationary points involved in this 13DC reaction, in gas phase are gathered in Table S3 in ESI,† while relative energies are included in Scheme 11. A schematic representation of the gas phase energy profiles for the four possible pathways is depicted in Fig. 5.

The activation energies associated with this 13DC reaction are 13.68 (**TS-d-mn**), 11.09 (**TS-d-mx**), 18.44 (**TS-d-on**), and 15.43 kcal mol^{-1} (**TS-d-ox**). We can notice that **TS-d-mx** is more favored by 2.59 kcal mol^{-1} than the second favoured approach (**TS-d-mn**) and by 4.34 kcal mol^{-1} than the more favoured *ortho* approach (**TS-d-ox**). These values accounts for a high *meta* regioselectivity and an *exo* stereoselectivity. Therefore, the present 13DC reaction favors the formation of a single stereoisomer which generated from *meta–exo* approach (**CA-d-mx**), in great agreement with our experimental observation.

The structures of the TSs implanted in the 13DC reaction of nitrone **1** with alkene **2d** are given in Fig. 4. For the *ortho* regioisomeric pathways, the lengths of the O–C and C–C new forming bonds are 2.09 and 2.05 Å at **TS-d-on**, 2.18 and 2.06 Å at **TS-d-ox**. For the favoured *meta* pathways, the lengths of the O–C and C–C newly formed bonds are 1.83 and 1.29 Å at **TS-d-mn** and 1.98 and 2.61 Å at **TS-d-mx**. Therefore, for the *ortho* pathways the formation of O–C and C–C were performed

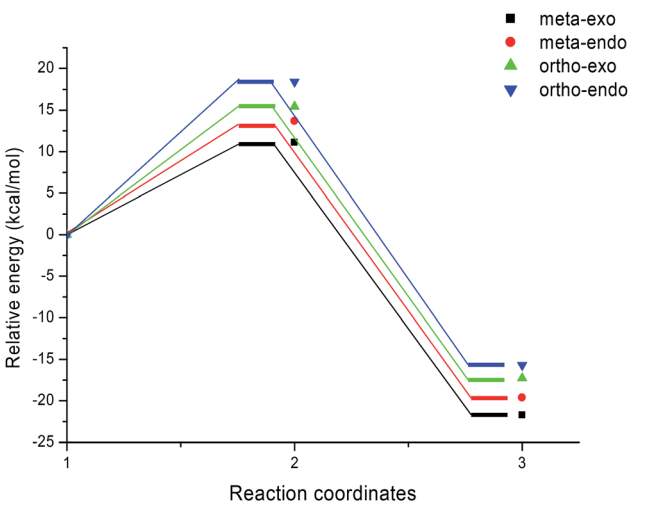

Fig. 5 Energy profiles for the 13DC reaction between nitrone **1** and alkene **2d**.

Table 3 B3LYP/6-31G(d) relative enthalpies (ΔH, in kcal mol^{-1}), entropies (ΔS, in cal mol^{-1}K^{-1}) and Gibbs free energies (ΔG, in kcal mol^{-1}), for the TSs and cycloadducts involved in the 32CA between nitrone **1** and alkene **2e**

	ΔH	ΔS	ΔG
TS-d-on	20.39	−46.97	38.40
TS-d-ox	16.96	−45.61	34.44
TS-d-mn	15.92	−45.56	33.38
TS-d-mx	13.07	−44.86	30.27
CA-d-on	−11.01	−48.64	7.64
CA-d-ox	−12.36	−47.74	5.94
CA-d-mn	−14.75	−48.46	3.83
CA-d-mx	−16.73	−47.27	1.39

synchronously. However, for the *meta* pathways, The formation of O–C and C–C were performed asynchronously; where, the new O–C σ bond was more advanced than the C–C one.

As the previous 13DC reaction, here also, we have evaluated the GEDT along these possible pathways using Natural Population Analysis (NPA).[16] The natural atomic charges at the TSs were calculated from the residual charge at the alkene **2d**. The negative sign of the GEDT indicate that the fluxes of GEDT occur from nitrone **1** toward alkene **2d**. Therefore, nitrone **1** will react as a nucleophile, whereas, alkene **2d** as an eletrophile. The values of GEDT are 0.06*e* at **TS-d-ox**, 0.03*e* at **TS-d-on**, 0.07*e* at **TS-d-mx** and 0.09*e* at **TS-d-mn**. These low values accounts for a non-polar character for this 13DC reaction.

The values of relative enthalpies, entropies and free energies associated to this 13DC reaction are collected in Table 3, while the values of total ones are gathered in Table S4 in ESI.†

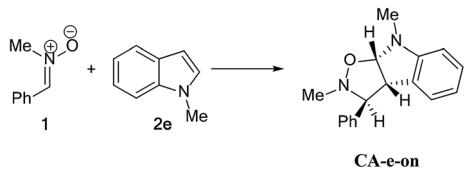

Scheme 12 13DC reaction between nitrone **1** and alkene **2e**.

A comparison between the activation enthalpy values indicated that the approach *meta–exo* is the more favoured reactive pathway, in agreement with the predicted activation energy. In addition, we notice that this 13DC reaction is entropically unfavourable due to bimolecular process. Thus, this 13DC reaction has activation entropy in the range from −46.97 to −44.86 cal mol^{-1} K^{-1}, thereby, the addition of thermal corrections and entropic contribution to the electronic energies increases the activation free energies by around 18 kcal mol^{-1}, which raises the free activation energy to 38.40 to 34.44, 33.38, 30.27 kcal mol^{-1} for **TS-d-on**, **TS-d-ox**, **TS-d-mn** and **TS-d-mx**, respectively. Therefore, these high values do not change the *meta–exo* selectivity, but it making this 13DC reaction slightly unfavourable. In addition, the obtained cycloadducts are more stables in comparison with these obtained in the 13DC reaction of nitrone **1** with alkene **2a**, which explain the experimental good yield.

2.2.3. Study of the 13DC reaction between nitrone 1 and alkene 2e. The 13DC reaction between nitrone **1** and alkene **2e** leading to the formation of a single cycloadduct was also studied (Scheme 12). Values of the total and relative phase gas energies of the stationary points involved in this 13DC reaction are given in Table S5 in ESI,† while relative ones are included in Scheme 13.

We can notice from Scheme 13 that the gas phase activation energies associated with the 13DC reaction between nitrone **1** and alkene **2e** are 25.09 (**TS-e-mn**), 23.27 (**TS-e-mx**), 19.47 (**TS-e-on**), and 18.63 kcal mol^{-1} (**TS-e-ox**), these values accounts for a complete *ortho* regioselectivity and an *exo* stereoselectivity (Fig. 6). On the other hand, the comparison between the cycloadducts energies shows that these products are less stables. This fact accounts for the irreversibility of this 13DC reaction. Thereby, this cycloaddition is under both kinetic and thermodynamic controls. Therefore, the present 13DC reaction favoring kinetically and thermodynamically the formation of a single stereoisomer **CA-e-ox**, in great agreement with experimental data.

The values of the relative enthalpies, entropies and Gibbs free energies of the TSs and cycloadducts involved in the

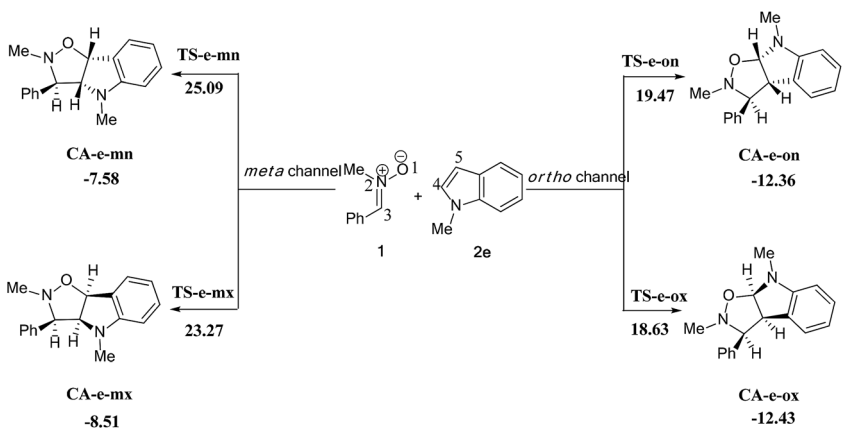

Scheme 13 The possible regio- and stereoisomeric pathways of the 13DC reaction between nitrone **1** and alkene **2e**.

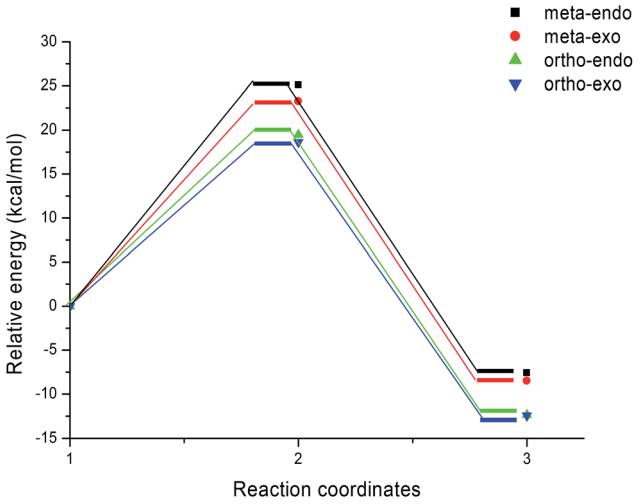

Fig. 6 Energy profiles for the 13DC reaction between nitrone **1** and alkene **2e**.

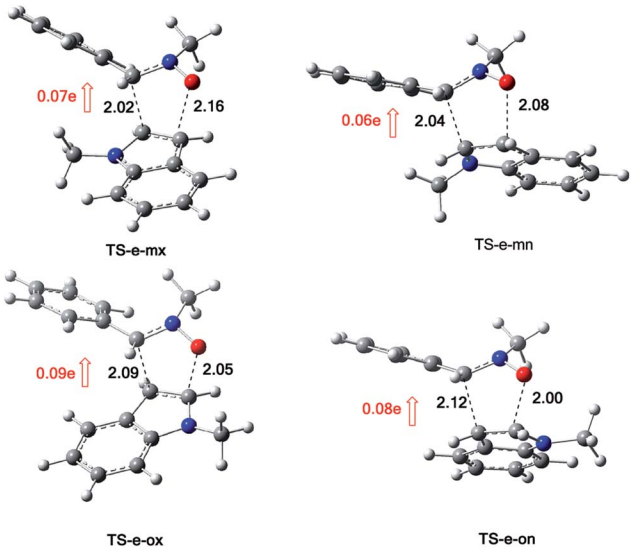

Fig. 7 Structure of TSs involved in the 13DC reaction between nitrone **1** and alkene **2e**.

reaction of nitrone **1** with alkene **2e** are collected in Table 4, while the total ones are given in Table S6 in ESI.†

From Table 2, a comparison between the relative activation enthalpies associated with the four reactive pathways of the 13DC reaction of nitrone **1** with alkene **2e** indicates that the most favourable approach mode is always that associated with **TS-e-ox** (ΔH = 21.04 kcal mol^{-1}). Addition of the entropic contribution to the enthalpy increases the activation Gibbs free energy of this reactive channel to 38.11 kcal mol^{-1}, as a consequence of the unfavourable negative activation entropy, ΔS = −53.9 cal mol^{-1} K^{-1}. Moreover, this 13DC reaction shows slightly endothermic character, which account for its reversibility, where **CA-e-ox** is favoured thermodynamically because it is the more stable cycloadduct. Consequently, it is expected to obtain a single isomer (**CA-e-ox**) from this 13DC reaction, as observed experimentally.

The structures of the TSs implanted in the 13DC reaction of nitrone **1** with alkene **2e** are illustrated in Fig. 7. For the favoured *ortho* regioisomeric pathways, the lengths of the O–C and C–C newly formed bonds are 2.05 and 2.09 Å at **TS-e-ox**, 2.00 and 2.12 Å at **TS-e-on**. For the *meta* pathways, the lengths of the O–C and C–C new forming bonds are 2.16 and 2.02 Å at **TS-e-mx** and 2.08 and 2.04 Å at **TS-e-mn**. Therefore, for both the *ortho* and *meta* pathways the formation of O–C and C–C were performed synchronously.

The evaluation of the GEDT along these 13DC paths is performed using NPA analysis.[16] The natural atomic charges at the TSs were shared between nitrone **1** and alkene **2e**. These values are calculated from the sum of the partial residual charge of the nitrone **1** atoms. The negative sign of GEDT indicates that the fluxes of the GEDT occur from alkene **2e** toward nitrone **1**. The values of GEDT are 0.09*e* at **TS-e-ox**, 0.08*e* at **TS-e-on**, 0.07*e* at **TS-e-mx** and 0.06*e* at **TS-e-mn**. These values indicate that this 13DC reaction has a low polar character, which account for a non-polar 13DC reaction and justifying the high activation energy.[17]

2.2.4. Analysis of reactivity indices derived from conceptual DFT. At the transition states, there is an electron density transfer from the nucleophile fragment toward the electrophile fragment, which is measured by the GEDT value.[16] The low value of the GEDT account for the non-polar reaction. In the literature, various studies have shown that there is a relationship between the polar character of the reactions and the nature of the reactants.[18] These studies indicates that the global reactivity indices are a powerful tools for study the feasibility of the reaction, as well as the reactivity of the reagents.[19] The global reactivity indices of nitrone **1**, alkenes **2a**, **2d** and **2e** are calculated and given in Table 5.

Table 4 B3LYP/6-31G(d) relative enthalpies (ΔH, in kcal mol^{-1}), entropies (ΔS, in cal mol^{-1} K^{-1}) and Gibbs free energies (ΔG, in kcal mol^{-1}), for the TSs and cycloadducts involved in the 13DC between nitrone **1** and alkene **2e**

System	ΔH	ΔS	ΔG
TS-e-mn	27.54	−45.48	44.97
TS-e-mx	25.02	−45.13	42.31
TS-e-on	22.31	−46.54	40.15
TS-e-ox	21.04	−44.56	38.11
CA-e-mn	−2.79	−47.26	15.31
CA-e-mx	−3.73	−47.50	14.47
CA-e-on	−7.35	−48.12	11.09
CA-e-ox	−7.30	−47.88	11.04

Table 5 Electronic chemical potential (μ), chemical hardness (η), global electrophilicity (ω) and global nucleophilicity (N), in eV, of nitrone **1** and alkenes **2a**, **2d** and **2e**

	HOMO	LUMO	μ	η	ω	N
Nitrone **1**	−5.49	−1.32	−3.41	4.17	1.39	4.00
Alkene **2a**	−6.58	−2.09	−4.33	4.49	2.09	2.91
Alkene **2d**	−6.38	−2.01	−4.19	4.37	2.01	3.11
Alkene **2e**	−5.13	−0.11	−2.62	5.03	0.68	4.36

The electronic chemical potential of nitrone **1**, $\mu = -3.41$ eV is higher than that of alkene **2a**, $\mu = -4.33$ eV and alkene **2d**, $\mu = -4.19$ eV. Thereby, during these 13DCs, the GEDT will takes place from nitrone **1** toward alkenes **2a** and **2b**. On the other hand, this value is lower of that of alkene **2e**, $\mu = -2.62$ eV, indicating that the GEDT will occur from alkene **2e** towards nitrone **1**, in great agreement with the GEDT calculated at the TSs.

The electrophilicity and nucleophilicity indices of nitrone **1** are $\omega = 1.39$ and $N = 4.00$ eV, allow its classification as a moderate electrophile and a strong nucleophile based on the electrophilicity[20] and nucleophilicity[21] scales. In addition, the electrophilicity and nucleophilicity indices of alkene **2a** are $\omega = 2.09$ and $N = 2.91$ eV, and for alkene **2b** are $\omega = 2.01$ and $N = 3.11$ eV, being classified as a moderate electrophiles and as a moderate nucleophiles. Therefore, nitrone **1** will react as a strong nucleophile and alkenes **2a** and **2d** as a moderate electrophiles. Consequently, these 13DC reactions will presents relatively moderate activation energy and proceeds *via* a slightly polar mechanism.

On the other hand, the electrophilicity and nucleophilicity indices of alkene **2e** are $\omega = 0.68$ and $N = 4.36$ eV, being classified as a marginal electrophile and as a strong nucleophile. Therefore, in the 13DC reaction between nitrone **1** and alkene **2e**, the dipole (nitrone **1**) will react as an electrophile and the dipolarophile (alkene **2e**) as a nucleophile. Tacking account that both nitrone **1** and alkene **2e** are a strong nucleophiles, this 13DC reaction will demand a strong experimental conditions, and proceeds *via* a non-polar mechanism and high activation energy, in agreement with experimental data and GEDT analysis, which allowing to explain the obtained low yield.

In order to predict the regioselectivity in cycloaddition reactions, recent studies indicates that the most favorable reactive channel is that implied the initial two-center interaction between the most electrophilic and nucleophilic centers of both reagents.[22] Recently, Domingo *et al.*[23] proposed the electrophilic P_k^+ and nucleophilic P_k^- Parr functions derived from the changes of spin electron-density occurred *via* the GEDT process from the nucleophile to the electrophile as powerful tools in the study of the local reactivity. Therefore, the electrophilic P_k^+ Parr functions for alkene **2a**, alkene **2d**, and nitrone **1** and the nucleophilic P_k^- Parr functions for alkene **2e** and nitrone **1** are analysed in order to predict the most favourable electrophile/nucleophile two-center interaction in these 13DC reactions and, accordingly to explain the regioselectivity observed experimentally.

The tridimensional (3D) maps of the atomic spin density (ASD) of both systems; the radical cation of nitrone **1** and alkene **2e** and the radical anion of alkene **2a**, alkene **2d** and nitrone **1**, including the values of nucleophilic Parr functions of nitrone **1** and alkene **2e** and the electrophilic Parr functions of alkene **2a**, alkene **2d** and nitrone **1** are given in Fig. 8.

From Fig. 8, we can notice that along these 13DC reactions, analysis of electrophilic Parr functions of alkenes **2a** and **2b** indicates that the C4 carbon atom (see Schemes 9 and 11 for atom numbering) is the most electrophilic one of these molecules, $P = 0.229$ for alkene **2a** and $P = 0.552$ for alkene **2b**. On the other hand, the nucleophilic Parr functions of nitrone **1** are mainly concentrated at the O1 oxygen atom ($P = 0.586$), account for a *meta* regioselectivity of these 13DC reactions. For the 13DC reaction between nitrone **1** and alkene **2e**, analysis of electrophilic Parr functions of nitrone **1** indicates that the C3 carbon atom is the most electrophilic center ($P = 0.189$). In addition,

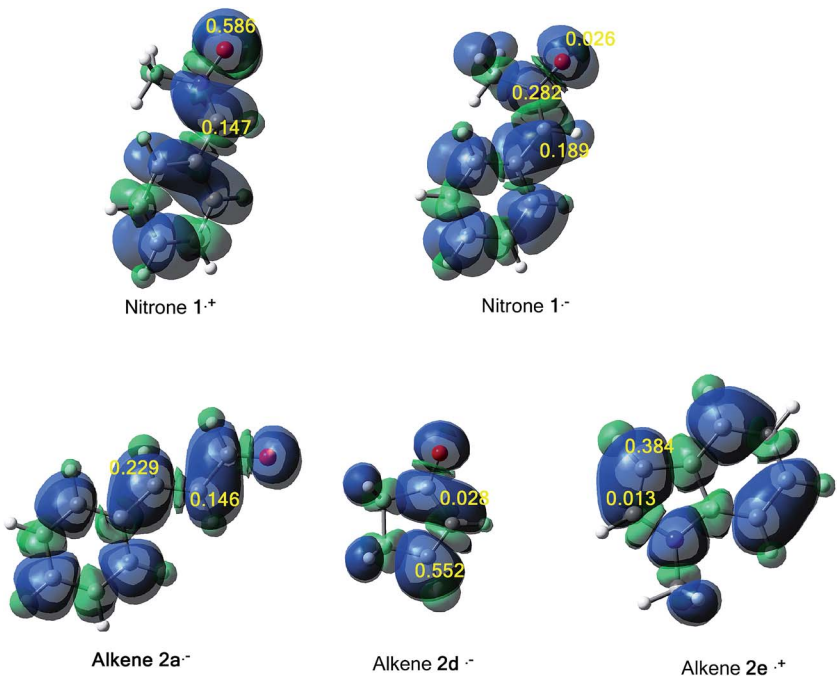

Fig. 8 3D Maps of ASD for cation radicals nitrone $\mathbf{1}^{\bullet+}$, alkene $\mathbf{2e}^{\bullet+}$ and anion radical nitrone $\mathbf{1}^{\bullet-}$ and alkene $\mathbf{2d}^{\bullet-}$ and alkene $\mathbf{2a}^{\bullet+}$ with the nucleophilic P_k^- of nitrone $\mathbf{1}^{\bullet+}$ and alkene $\mathbf{2e}^{\bullet+}$ and electrophilic P_k^+ Parr functions for nitrone $\mathbf{1}^{\bullet-}$, alkene $\mathbf{2a}^{\bullet+}$ and alkene $\mathbf{2d}^{\bullet-}$.

for the alkene **2e**, the most nucleophilic center is located at the C5 atom (see Scheme 13 for atom numbering). Thereby, the most favourable nucleophilic/electrophilic interaction will occur between C3 carbon atom of nitrone **1** and C5 atom of alkene **2e** leading to the formation of the *ortho* regioisomers, in good agreement with the experimental outcome.

3. Conclusions

In this work, we have investigated experimentally and theoretically the regio- ans stereoselectivities of the 1,3-dipolar cycloaddition of *C*-phenyl-*N*-methylnitrone with different substituted alkenes.

For the synthesis of isoxazolidines, the pure products were purified using chromatography technique and the structures were determined using spectroscopic methods. The principal conclusions are the followings:

(a) The 13DC reactions of nitrone **1** with alkenes **2a**, **2b** and **2d** are completely regioselective and stereoselective leading to the formation of the cycloadduct generated from *meta–endo* and *meta–exo* approaches, respectively.

(b) The 13DC reaction between nitrone **1** and alkene **2c** is completely regioselective but it has a poor stereoselectivity leading to the formation of a mixture of both *meta–endo* and *meta–exo* cycloadducts in a ratio of 80/20.

(c) The 13DC reactions of nitrone **1** with alkene **2e** are completely regioselective and stereoselective leading to the formation of the cycloadduct generated from *ortho–exo* approach.

For the theoretical investigation, we have performed a computational study of the mechanism and the regio- and stereoselectivities of the 13DC reactions of nitrone **1** with alkenes **2a**, **2d** and **2e** using DFT methods at the B3LYP/6-31G(d) theoretical level. The main conclusions which can be extracted from our results are the following:

(i) The 13DC reaction of nitrone **1** with alkene **2e** is completely *ortho*-regioselective and an *exo* stereoselective leading kinetically and thermodynamically to the formation of a single diastereoisomer **CA-e-ox**, in a low yield.

(ii) The 13DC reactions of nitrone **1** with alkenes **2a** and **2d** is completely *meta* regioselective and an *endo* stereoselective for the alkene **2a** and *exo* stereoselective for the alkene **2d**, leading kinetically and thermodynamically to the formation of a single diastereoisomer **CA-a-mn** and **CA-d-mx**, respectively, in a great agreement with experimental observations.

(iii) An analysis of the relative free energies of the TSs involved in these 13DCs reveals that the inclusion of the thermal corrections and entropic contribution to the electronic energies does not modify the selectivity found with the gas-phase electronic energies. The main change is the increase of the activation energies, as a consequence of the negative values of entropies associated with the bimolecular character of these 13DC reactions.

(iv) The endothermic character account for the reversibility of these 13DC reactions, which reveals that they also under thermodynamic control, in which the kinetic product is also favoured thermodynamically.

(v) Analysis of GEDT and geometries of TSs indicates that these 13DC reactions proceed *via* a non-polar synchronous mechanism for the 13DC reaction between nitrone **1** and alkene **2e**, as a consequence of the nucleophilic character of both reagents. For the 13DC reaction between nitrone **1** and alkenes **2a** and **2d**, the favorable *meta* paths proceeds with an asynchronous non-polar mechanism and a relatively low activation energies, as a consequence for the electrophilic character of both alkene **2a** and alkene **2d**.

(vi) Analysis of the DFT reactivity indices at the ground state of the reagents involved in these 13DC reactions indicates that both nitrone **1** and alkene **2e** are a strong nucleophile and alkenes **2a** and **2d** are a good electrophiles which explain the obtained activation energies and the polar character of these 13DC reactions.

(vii) The analysis of local reactivity indices based on Parr functions method predicts correctly the regioselectivity observed experimentally.

(viii) The present study suggests that the electronic and steric effects have an important role in the determination of the regioselectivity and the stereoselectivity, as well as the reactivity of the regents.

4. Experimental section

4.1. General

All reactions were carried out in dried reaction glassware under argon, using a parallel reactor that will allow us to run multiple reactions simultaneously and under the same conditions; same temperature and same stirring speed. The temperatures of the reaction are reported as the temperature of the hot plate used. The commercial products were obtained from Sigma Aldrich, Alfa Aesar and was typically used without further purification except the reagent *trans*-cinnamaldehyde **2a** and toluene solvent which were used freshly distilled. The spectra of ^{1}H NMR, ^{13}C NMR, cosy (2D: ^{1}H–^{1}H) and HMQC (2D: ^{1}H–^{13}C) were recorded on a Bruker Ultra shield 400 MHz. Chemical shifts (δ) are expressed on parts per million (ppm) relative to external reference TMS. Coupling constants (J) are given in hertz. The NMR spectra were performed in $CDCl_3$ and referenced to the residual peak of $CHCl_3$ at δ_H = 7.26 ppm and δ_C = 77.00 ppm for ^{1}H and ^{13}C, respectively. Infrared spectra (IR) were recorded with a spectrometer Perkin Elem spectrum 1000. Mass spectra and high-resolution mass spectra were obtained from the mass spectrometer operated by the Laboratory of Physics Measurement of the University Montpellier 2. All the reactions were monitored by thin-layer chromatography (TLC) on silica gel 60 F_{254} TLC plates; the revelation was attended up with UV light, and a colored solution of potassium permanganate or a ninhydrin solution followed by simple heating. Chromatography was carried out with silica gel 60 A (35–70 μm). Petroleum ether and ethyl acetate were used as eluent for purification with column chromatography.

4.2. Procedure for the synthesis of nitrone 1

In a ball bicol of 250 ml under magnetic stirring, the benzaldehyde (0.02 mol) was dissolved in an anhydrous toluene, then

the *N*-methylhydroxylamine hydrochloride (CH_3NHOH, HCl) (0.02 mol), was added. When the refluxing began, a solution of triethylamine (NEt_3) (0.02 mol) dissolved in dry toluene was added dropwise using a dropping funnel. The reaction mixture is brought to refluxed toluene for 2 hours. We use a Dean Stark for removing the water molecules, which generated during the reaction. Once the reaction is completed, the mixture is immersed in an ice bath, the precipitate removed by vacuum filtration, the solvent was evaporated under reduced pressure. The crude product was purified by re-crystallization in diethyl ether. The nitrone **1** was separated by filtration as crystals. The characterization data and spectroscopic detail for the nitrones **1** are given in ESI.†

4.3. General procedure for the synthesis of isoxazolidines heterocycles 3a–e

An equimolecular amount (1 mmol) of the alkene and the nitrone **1** was introduced on tube of a parallel reactor and dissolved in anhydrous toluene (5 ml) under argon atmosphere. The mixture was refluxed of the solvent with stirring. The reaction evolution was monitored by TLC. After completion of the reaction, the reaction mixture was then cooled to room temperature, evaporated of solvent under reduced pressure. The crude product was purified by column chromatography (silica gel) which afforded the corresponding isoxazolidines. The reported yields were determined based on the isolated pure products and in the case of the mixture, the relative proportions were determined from ^{1}H NMR spectrum.

4.4. Characterization data and spectroscopic detail for the obtained compounds

4.4.1. Reaction of nitrone 1 with alkene 2a. Reaction of nitrone **1** with alkene **2a** afforded isoxazolidine **3a** as a single regio- and stereoisomer (**CA-a-mn**). This compound was prepared according to general procedure as described above. The resulting crude product was purified by silica gel column chromatography (petroleum ether : ethyl acetate 80 : 20 eluent) afforded **3a** as brick red oil in 10% yield as one diastereoisomer (**CA-a-mn**). R_f = 0.29 (petroleum ether : ethyl acetate: 80 : 20 eluent). ^{1}H NMR ($CDCl_3$, 400 MHz): δ 2.70 (s, 3H, N–C**H**$_3$), δ 2.56 (m, 1H, C4–**H**), δ 4.32 (d, J = 3.68 Hz, 1H, C3–**H**), δ 5.37 (d, J = 5.8 Hz, 1H, C5–**H**), δ 7.27–7.35 (m, 10H, H$_{arom}$), δ 9.85 (s, 1H, C**H**O). ^{13}C NMR ($CDCl_3$, 400 MHz): δ 42.70 (N–CH_3), 44.52 (**C**3), 61.24 (**C**4), 62.5 (**C**5), 125.73 (**C**$_{arom}$), 127.73 (**C**$_{arom}$), 127.81 (**C**$_{arom}$), 128.31 (**C**$_{arom}$), 128.77 (**C**$_{arom}$), 128.85 (**C**$_{arom}$), 128.92 (**C**$_{arom}$), 129.04 (**C**$_{arom}$), 135 (**C**HO). IR (thin film): 2832, 1827, 1660, 1340, 1040 cm^{-1}. HRMS (ESI$^+$): m/z calcd for $[C_{17}H_{17}NO_2 + H]^+$: 268.1338; found 268.1337.

4.4.2. Reaction of nitrone 1 with alkene 2b. This 13DC reaction afforded isoxazolidines **3b** which was prepared according to general procedure described previously. The resulting crude product was purified by column chromatography (silica gel, PE/AcOEt: 80 : 20) given **3b** as red oil in 12% yield as a single regio- and stereoisomer (**CA-b-mn**). R_f = 0.17 (petroleum ether : ethyl acetate: 80 : 20 eluent). ^{1}H NMR ($CDCl_3$, 400 MHz): δ 1.25 (s, 3H, C**H**$_3$), δ 3.18 (q, 1H, C4–**H**), δ 3.80 (s, 3H, O–C**H**$_3$), δ 4.68 (d, J = 5.6 Hz, 1H, C3–**H**), δ 6.05 (d, J = 14.4 Hz, 1H, C5–**H**), δ 6.84 (m, 2H, C**H**$_{arom}$), δ 7.03–7.36 (m, 7H, C**H**$_{arom}$), δ 8.42 (s, 1H, C**H**O). ^{13}C NMR ($CDCl_3$, 100 MHz): δ 38.67 (N–**C**H_3), 55.35 (O–**C**H_3), 70.53 (**C**4), 72.98 (**C**5), 80.94 (**C**3), 110.86 (**C**$_{arom}$), 114.22 (**C**$_{arom}$), 114.29 (**C**$_{arom}$), 126.63 (**C**$_{arom}$), 127.02 (**C**$_{arom}$), 150 (**C**$_{arom}$), 190.36 (**C**HO) IR (thin film): 2830, 1720, 1550, 1135, 1018 cm^{-1}. HRMS (ESI$^+$): m/z calcd for $[C_{18}H_{19}NO_3 + H]^+$: 298.1443; found 298.14.

4.4.3. Reaction of nitrone 1 with alkene 2c. Reaction of nitrone **1** with alkene **2c** afforded isoxazolidine **3c**. The title compound was prepared according to general procedure as described above. The resulting crude product was purified by column chromatography (silica gel, PE/AcOEt: 80/20 eluent) to give **3c** in 49% yield as one regioisomer in two diastereoisomers (**CA-c-mn** and **CA-c-mx**) were initially present in an 80 : 20 of ratio, respectively, but only one diastereoisomer was isolated as an yellow oil. R_f = 0.44 (PE/AcOEt eluent: 80 : 20). ^{1}H NMR ($CDCl_3$, 400 MHz): δ 2.73 (s, 3H, N–C**H**$_3$), δ 3.38 (m, 1H, C4–**H**), δ 3.84 (d, J = 8.4 Hz, 1H, C3–**H**), δ 5.90 (d, J = 12 Hz, 1H, C5–**H**) for **CA-c-mn**, δ 5.95 (d, J = 4 Hz, 1H, C5–**H**) for **CA-c-mx**, δ 7.28 (m, 5H, H$_{arom}$), δ 7.47 (m, 1H, H$_{arom}$), δ 7.75 (m, 1H, H$_{arom}$), δ 8.14 (d, J = 1.2 Hz, 1H, H$_{arom}$), δ 8.33 (d, J = 8 Hz, 1H, H$_{arom}$), δ 10.02 (d, J = 2.4 Hz, 1H, C**H**O), ^{13}C NMR ($CDCl_3$, 400 MHz): δ 42.3 (N–CH_3), 72.20 (**C**5), 74.65 (**C**5), 76.15 (**C**3), 124.91 (**C**$_{arom}$), 127.84 (**C**$_{arom}$), 128.40 (**C**$_{arom}$), 128.53 (**C**$_{arom}$), 128.93 (**C**$_{arom}$), 129.04 (**C**$_{arom}$), 134.34 (**C**$_{arom}$), 136.35 (**C**$_{arom}$), 139.45 (**C**$_{arom}$), 198.14 (**C**HO). IR (thin film): 2850, 1726, 1521, 1345, 1302 cm^{-1}. HRMS (ESI$^+$): m/z calcd for $[C_{17}H_{16}N_2O_4 + H]^+$: 313.1188; found 313.1192.

4.4.4. Reaction of nitrones 1 with alkene 2d. The reaction of nitrone **1** with alkene **2d** afforded isoxazolidine **3d**. The title compound was prepared according to general procedure as described above. The resulting crude product was purified by column chromatography (silica gel, PE/AcOEt: 85 : 15) to give **3d** in 90% yield as a single regio- and diastereoisomer (**CA-d-mx**). R_f = 0.26 (PE : AcOEt: 85 : 15 eluent) as yellow oil. ^{1}H NMR ($CDCl_3$, 400 MHz): δ 1.97 (m, 2H, C**H**$_2$), δ 2.01 (m, 2H, C**H**$_2$), δ 2.54 (s, 3H, N–C**H**$_3$), δ 2.90 (t, 1H, C4–**H**), δ 3.42 (d, J = 5.6 Hz, 1H, C3–**H**), δ 4.86 (q, 1H, C5–**H**), δ 7.17 (m, 5H, **H**$_{arom}$). ^{13}C NMR ($CDCl_3$, 400 MHz): δ 24.14 (**C**H_2), 29.66 (**C**H_2), 35.24 (N–**C**H_3), 42.89 (**C**4), 64.94 (**C**5), 77.56 (**C**3), 127.66 (C$_{arom}$), 127.74 (C$_{arom}$), 128.03 (C$_{arom}$), 128.42 (C$_{arom}$), 138.84 (C$_{arom}$), 217.83 (**C**=O). IR (thin film): 2848.83, 1736, 1154.64 cm^{-1}. HRMS (ESI$^+$): m/z calcd for $[C_{13}H_{15}NO_2 + H]^+$: 218.1181; found 218.1186.

4.4.5. Reaction of nitrone 1 with alkene 2e. The reaction of nitrone **1** with alkene **2e** afforded isoxazolidines **3e**. The title compound was prepared according to general procedure as described above. The obtained crude product was purified by column chromatography (silica gel, PE/AcOEt: 85 : 15) to give **3e** in 23% yield as one diastereoisomer. R_f = 0.36 (PE/AcOEt: 85/15) as pink oil. ^{1}H NMR ($CDCl_3$, 400 MHz): δ 3.68 (s, 3H, N–C**H**$_3$), δ 3.71 (s, 3H, N–C**H**$_3$), δ 3.86 (d, J = 10.8 Hz, 1H, C4–**H**), δ 4.21 (d, J = 0 Hz, 1H, C3–**H**), δ 5.82 (d, J = 0 Hz, 1H, **H**$_{arom}$), δ 6.52 (s, 1H, **H**$_{arom}$), δ 6.80 (t, 1H, **H**$_{arom}$), δ 7.19 (m, 2H, **H**$_{arom}$), δ 7.29 (m, 5H, **H**$_{arom}$). ^{13}C NMR ($CDCl_3$, 400 MHz): δ 29.71 (N–**C**$H_{3indole}$), 32.57 (N–**C**H_{3isoxa}), 51.43 (**C**4), 80.00 (**C**3), 109.03 (C5), 118.62 (C$_{arom}$), 120.03 (C$_{arom}$), 121.40 (C$_{arom}$), 126.00 (C$_{arom}$), 128.25 (C$_{arom}$), 135.12 (C$_{arom}$), 136.31 (C$_{arom}$), 148.64 (C$_{arom}$). IR (thin film):

3110, 3015, 1660, 1545 cm^{-1}. HRMS (ESI^+): *m*/*z* calcd for $[C_{19}H_{17}N_2O + H]^+$: 289.1341; found 289.1340.

5. Computational methods

The structures of all systems involved in these 13DC reactions were optimized using the B3LYP[24] functional together with the 6-31G(d) basis set.[25] The nature of the stationary points were confirmed by frequency calculations in order to distinguished between the minimums and transition states, which have zero and one imaginary frequency, respectively. The electronic structures of the TSs were analyzed by the natural bond orbital (NBO) method.[26] Values of enthalpies, entropies, and Gibbs free energies in chloroform were calculated with standard statistical thermodynamics at 383 K and 1 atmosphere over the optimized gas-phase structures[27] All computations were carried out with the Gaussian 09 suite of programs.[28]

The global electrophilicity index,[29] ω, is given by the following expression, $\omega = (\mu^2/2\eta)$, in terms of the electronic chemical potential μ and the chemical hardness η. Both quantities may be approached in terms of the one-electron energies of the Frontier molecular orbitals HOMO and LUMO, ε_H and ε_L, as $\mu \approx (\varepsilon_H + \varepsilon_L)/2$ and $\eta = (\varepsilon_L - \varepsilon_H)$, respectively.[30] The empirical (relative) nucleophilicity index,[31] *N*, based on the HOMO energies obtained within the Kohn–Sham scheme,[32] is defined as $N = \varepsilon_{HOMO(Nu)} - \varepsilon_{HOMO(TCE)}$, where tetracyanoethylene (TCE) is the reference because it presents the lowest HOMO energy in a long series of molecules already investigated in the context of polar organic reactions. The electrophilic P_k^+ and nucleophilic P_k^- Parr functions[22] were obtained through the analysis of the Mulliken atomic spin densities (ASD) of the corresponding radical anion and radical cation by single-point energy calculations over the optimized neutral geometries.

Acknowledgements

This work was supported by the Ministry of Higher Education and Scientific Research of the Algerian Government [project CNEPRU Code: E01620140051].

References

1 R. Huisgen, in *1,3-Dipolar Cycloaddition Chemistry*, ed. A. Padwa, John Wiley & Sons, New York, 1984, vol. 1, pp. 42–47.
2 J. N. Martin and R. C. Jons, Nitrones, in *Synthetic Applications of 1,3-Dipolar Cycloaddition. Chemistry Towards Heterocycles and Natural Products*, ed. A. Padwa and W. H. Pearson, John Wiley & Sons, Hoboken, NJ, 2003, ch. 1.
3 (*a*) M. Frederickson, *Tetrahedron*, 1997, **53**, 403–425; (*b*) K. V. Gothelf and K. A. Jorgensen, *Chem. Rev.*, 1998, **98**, 863–909.
4 J. P. G. Seerden, M. M. M. Boeren and H. W. Scheeren, *Tetrahedron*, 1997, **53**, 11843.
5 (*a*) W. Patterson, P. S. Cheung and M. J. Ernest, *J. Med. Chem.*, 1992, **35**, 507; (*b*) E. Wagner, L. Becan and E. Nowakowska, *Bioorg. Med. Chem.*, 2004, **12**, 265.
6 (*a*) U. Chiacchio, F. Casuscelli, A. Cocsaro, A. Rescifina, G. Romeo and N. Uccella, *Tetrahedron*, 1994, **50**, 6671–6680; (*b*) M. Bakavoli, F. Moeinpour, A. Davoodnia and A. Morsali, *J. Mol. Struct.*, 2010, **969**, 139–144; (*c*) K. V. Gothelf and K. A. Jørgensen, *Chem. Commun.*, 2000, 1449–1458; (*d*) F. Chafaa, D. Hellel, A. K. Nacereddine and A. Djerourou, *Tetrahedron Lett.*, 2016, **57**, 67–70.
7 T. Q. Tran, V. V. Diev and A. P. Molchanov, *Tetrahedron*, 2011, **67**, 2391.
8 A. K. Nacereddine, C. Sobhi, A. Djerourou, M. Ríos-Gutiérrez and L. R. Domingo, *RSC Adv.*, 2015, **5**, 99299.
9 E. Falkowska, M. Y. Laurent, V. Tognetti, L. Joubert, P. Jubault, J. Bouillon and X. Pannecoucke, *Tetrahedron*, 2015, **71**, 8067–8076.
10 K. N. Houk, *Acc. Chem. Res.*, 1975, **8**, 361.
11 (*a*) R. G. Parr and W. Yang, *J. Am. Chem. Soc.*, 1984, **106**, 4049; (*b*) L. R. Domingo, M. J. Aurell, P. Pérez and R. Contreras, *J. Phys. Chem. A*, 2002, **106**, 6871–6875.
12 H. Eyring, *J. Chem. Phys.*, 1935, **3**, 107.
13 P. Geerlings, F. De Proft and W. Langenaeker, *Chem. Rev.*, 2003, **103**, 1793; D. H. Ess, G. O. Jones and K. N. Houk, *Adv. Synth. Catal.*, 2006, **348**, 2337.
14 R. C. F. Jones and J. N. Martin, in *Synthetic Applications of 1,3-Dipolar Cycloaddition Chemistry Toward Heterocycles and Natural Products*, A. Padwa and W. H. Pearson, John Wiley & Sons, New York, NY, 2002, pp. 1–81.
15 (*a*) M. P. S. Ishar, G. Singh, K. Kumar and R. Singh, *Tetrahedron*, 2000, **56**, 7817; (*b*) G. Singh, M. P. S. Ishar, N. K. Girdhar and L. Singh, *J. Heterocycl. Chem.*, 2005, **42**, 1047; (*c*) R. Huisgen, H. Hauck, H. Seidl and M. Burger, *Chem. Ber.*, 1969, **102**, 1117; (*d*) R. Sustmann, R. Huisgen and H. Huber, *Chem. Ber.*, 1967, **100**, 1802.
16 (*a*) A. E. Reed, R. B. Weinstock and F. Weinhold, *J. Chem. Phys.*, 1985, **83**, 735; (*b*) A. E. Reed, L. A. Curtiss and F. Weinhold, *Chem. Rev.*, 1988, **88**, 899.
17 L. R. Domingo, M. J. Aurell and P. Pérez, *Tetrahedron*, 2014, **70**, 4519.
18 (*a*) P. Geerlings, F. De Proft and W. Langenaeker, *Chem. Rev.*, 2003, **103**, 1793; (*b*) M. Ríos-Gutiérrez, F. Chafaa, A. K. Nacereddine, A. Djerourou and L. R. Domingo, *J. Mol. Graphics Modell.*, 2016, **70**, 296–304.
19 L. R. Domingo and J. A. Sáez, *Org. Biomol. Chem.*, 2009, **7**, 3576.
20 L. R. Domingo, M. J. Aurell, P. Pérez and R. Contreras, *Tetrahedron*, 2002, **58**, 4417.
21 P. Jaramillo, L. R. Domingo, E. Chamorro and P. Pérez, *J. Mol. Struct.*, 2008, **865**, 68.
22 (*a*) A. Ghomri and S. M. Mekelleche, *Mol. Phys.*, 2014, **112**, 566; (*b*) L. R. Domingo and P. Pérez, *Org. Biomol. Chem.*, 2013, **11**, 4350; (*c*) L. R. Domingo and S. R. Emamian, *Tetrahedron*, 2014, **70**, 1267; S. Bouacha, A. K. Nacereddine and A. Djerourou, *Tetrahedron Lett.*, 2013, **54**, 4030. ; R. Jasinski, *Tetrahedron*, 2013, **69**, 927. (*d*) F. Chafaa, D. Hellel, A. K. Nacereddine and A. Djerourou, *Mol. Phys.*, 2016, **114**, 663.
23 L. R. Domingo, P. Pérez and J. A. Saez, *RSC Adv.*, 2013, **3**, 1486.

24 (*a*) C. Lee, W. Yang and R. G. Parr, *Phys. Rev. B: Condens. Matter Mater. Phys.*, 1988, **37**, 785; (*b*) A. D. Becke, *J. Chem. Phys.*, 1993, **98**, 5648.
25 W. J. Hehre, L. Radom, P. V. R. Schleyer, and J. A. Pople, *ab initio Molecular Orbital Theory*, Wiley, New York, 1986.
26 (*a*) A. E. Reed, R. B. Weinstock and F. Weinhold, *J. Chem. Phys.*, 1985, **83**, 735; (*b*) A. E. Reed, L. A. Curtiss and F. Weinhold, *Chem. Rev.*, 1988, **88**, 899.
27 A. D. Becke, *J. Chem. Phys.*, 1993, **98**, 5648.
28 M. J. Frisch, G. W. Trucks, H. B. Schlegel, G. E. Scuseria, M. A. Robb, J. R. Cheeseman, G. Scalmani, V. Barone, B. Mennucci, G. A. Petersson, H. Nakatsuji, M. Caricato, X. Li, H. P. Hratchian, A. F. Izmaylov, J. Bloino, G. Zheng, J. L. Sonnenberg, M. Hada, M. Ehara, K. Toyota, R. Fukuda, J. Hasegawa, M. Ishida, T. Nakajima, Y. Honda, O. Kitao, H. Nakai, T. Vreven, J. A. Montgomery, J. E. Peralta Jr, F. Ogliaro, M. Bearpark, J. J. Heyd, E. Brothers, K. N. Kudin, V. N. Staroverov, R. Kobayashi, J. Normand, K. Raghavachari, A. Rendell, J. C. Burant, S. S. Iyengar, J. Tomasi, M. Cossi, N. Rega, J. M. Millam, M. Klene, J. E. Knox, J. B. Cross, V. Bakken, C. Adamo, J. Jaramillo, R. Gomperts, R. E. Stratmann, O. Yazyev, A. J. Austin, R. Cammi, C. Pomelli, J. W. Ochterski, R. L. Martin, K. Morokuma, V. G. Zakrzewski, G. A. Voth, P. Salvador, J. J. Dannenberg, S. Dapprich, A. D. Daniels, O. Farkas, J. B. Foresman, J. V. Ortiz, J. Cioslowski, and D. Fox, *J. Gaussian 09*, Gaussian, Wallingford, CT, 2009.
29 R. G. Parr, L. V. Szentpaly and S. Liu, *J. Am. Chem. Soc.*, 1999, **121**, 1922.
30 (*a*) R. G. Parr and R. G. Pearson, *J. Am. Chem. Soc.*, 1983, **105**, 7512; (*b*) R. G. Parr and W. Yang, *Density Functional Theory of Atoms and Molecules*, Oxford University Press, New York, 1989.
31 (*a*) L. R. Domingo, E. Chamorro and P. Perez, *J. Org. Chem.*, 2008, **73**, 4615; (*b*) L. R. Domingo and P. Pérez, *Org. Biomol. Chem.*, 2011, **9**, 7168.
32 W. Kohn and L. J. Sham, *Phys. Rev.*, 1965, **140**, 1133.